Investigation of Laser Grooving for Composite Materials

G. Chryssolouris (2), P. Sheng, W. C. Choi; Laboratory for Manufacturing and Productivity, M.I.T., Cambridge, MA/USA
Received on January 18, 1988

An analysis of the laser grooving process was conducted for several composite materials. An analytical model was developed to determine groove depth from process parameters and thermal properties of the material. Experimental measurements of groove depth, groove width and damage width were taken for variations in scanning velocity, beam power, and beam passes. A close agreement was found between model predictions and experimental results for groove depths in carbon/teflon. Model predictions consistently overestimated depth values for glass-fiber composites, and correction for heat losses was added to the model to improve agreement with data. Glass/polyester also showed differences in groove depth, width and damage width for variations in beam scanning direction relative to fiber orientation. The groove width and damage width results for all three materials were compared with surface quality standards for laser cutting of composites.

KEY WORDS: Laser machining, laser cutting, composites machining, laser grooving model.

NOMENCLATURE

a: absorptivity
α: thermal diffusivity
c_p:specific heat
d: laser beam diameter
D: groove depth
δ: thermal penetration depth
ED:energy density
ϕ: y-axis groove slope
J: intensity of the laser beam
k: thermal conductivity
L: latent heat of vap.
λ: number of passes
n: unit normal
P: laser power
ρ: density
s: groove depth
s_+: previous depth
θ: x-axis groove slope
T_{vap}: vap. temp.
v: scanning velocity

INTRODUCTION

Lasers have found widespread industrial applications in cutting, drilling and scribing processes with a large variety of materials, especially fiber reinforced composites. Due to the abrasive characteristics of fiber materials, processing composites with traditional machining methods is difficult. Laser machining, however, is a non-contact process. A new concept for three-dimensional material removal is proposed, utilizing two intersecting laser beams to remove a volume of material [1,2]. Unlike through-cutting techniques, each beam creates a blind kerf in the workpiece. A material volume is removed when the two kerfs intersect. Of particular interest is the laser grooving process, where a blind kerf is formed by a single beam through single or multiple passes over a material surface. Major issues in this analysis are the material removal rate, surface quality and dimensional accuracy [3,4]. Material removal and surface quality are both related to process parameters, such as beam power, scanning velocity, and scanning direction.

Several recent investigations have been performed on laser cutting and drilling operations for polyester matrix materials [11] and aramid and graphite-reinforced materials [8]. In [11], a one-dimensional model of a semi-infinite composite body (with homogeneous material properties) interacting with the vaporized material was introduced. In [9,10] a laser grooving model for single-pass beam interaction with a homogeneous material was developed.

The main objectives of this investigation are to present an analytical model for "blind-cutting" of composite materials, perform an experimental study of groove depth and surface quality on three representative composite materials, and determine the degree and range of accuracy between model prediction and experimental results.

THEORETICAL ANALYSIS

A schematic of the grooving geometry for multiple beam passes is shown in Figure 1. A small control volume at an arbitrary point on the groove surface (with the groove surface inclined at an angle θ from the x axis and ϕ from the y axis) is chosen. The overall groove shape is modeled as piecewise linear. Energy is introduced into the control volume as beam intensity and balanced by material ablation and heat conduction, as shown by the relation:

$$aJ(dxdy) = -k\left(\frac{dxdy}{\cos\theta\cos\phi}\right)\left(\frac{\partial T}{\partial n}\right)_{n=0} + \rho Lv(dxdy)\tan\theta \qquad (1)$$

Several assumptions are made for this analysis. First, the thermal properties used are the volume fraction averages of the matrix and fiber material values. Second, beam-material interaction results in material removal at the vaporization temperature. Material removal occurs in two modes. The majority of material is removed through vaporization [9]. A thin band of material (dependent on the thermal diffusivity of the material and effects of the assist gas), however, exists in the molten state between vaporization and melting temperatures. The molten material is entirely removed with the aid of a gas jet and does not affect the beam-material interaction.

Third, conduction into the workpiece occurs normal to the groove surface, resulting in a normal temperature distribution:

$$T = T_s\left(1 - \frac{n}{\delta}\right)^2 \qquad (2)$$

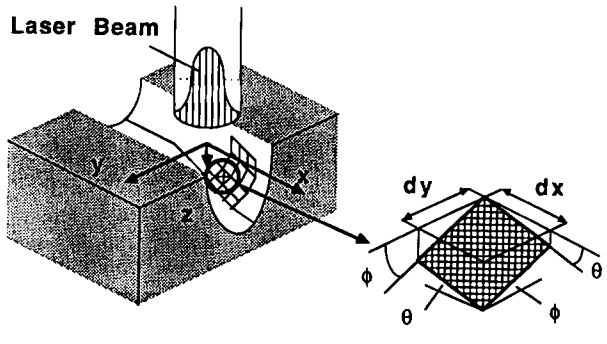

Figure 1: Groove Surface Control Volume

Fourth, the laser beam has a Gaussian intensity distribution:

$$J = \frac{P}{d^2}\exp\left(-\frac{x^2+y^2}{d^2}\right) \qquad (3)$$

From the above assumptions, the temperature gradient at the groove surface can be derived:

$$\left(\frac{\partial T}{\partial n}\right)_{n=0} = 2T_s\left(1-\frac{n}{\delta}\right)_{n=0}\left(-\frac{1}{\delta}\right) = -\frac{2T_s}{\delta} \qquad (4)$$

Substitution of this relationship into Eq. (1) yields:

$$aJ = \frac{2kT_s}{\delta \cos\theta \cos\phi} + \rho v L \tan\theta \quad (5)$$

A relationship between heat conduction into the workpiece and heat transfer due to motion of the heat source can be derived from the differential heat transfer equation:

$$\frac{v}{\alpha}\frac{\partial T}{\partial x} = \nabla^2 T = \frac{\partial^2 T}{\partial n^2} \quad (6)$$

Also, the temperature gradient can be expressed as:

$$\left(\frac{\partial T}{\partial x}\right)_{n=0} = -\left(\frac{\partial T}{\partial n}\right)_{n=0} \sin\theta \quad (7)$$

Solution of the energy equation (Eq. (1)) at the groove surface yields:

$$\frac{v}{\alpha}\frac{2T_s}{\delta}\sin\theta = \frac{2T_s}{\delta^2} \quad (8)$$

and a solution for δ is:

$$\delta = \frac{\alpha}{v \sin\theta} \quad (9)$$

Substitution for penetration depth into Eq. (5) yields:

$$aJ = \rho v \tan\theta \,(2c_p T_s \sec\phi + L) \quad (10)$$

Substitution of a Gaussian profile for J gives:

$$\tan\theta = \frac{\frac{aP}{d^2}\exp\left(-\frac{x^2+y^2}{d^2}\right)}{\rho v\,(2c_p T_s \sec\phi + L)} \quad (11)$$

Integration from $-\infty$ to x gives the groove depth:

$$s(x,y) = \int_{-\infty}^{x} ds + s_+ \quad (12)$$

where s_+ is the previous groove depth and ds is the change in groove depth during the current beam pass. The integral relationship for the groove depth becomes:

$$s(x,y) = \int_{-\infty}^{x} \frac{\frac{aP}{d^2}\exp\left(-\frac{x^2+y^2}{d^2}\right)}{\rho v(2c_p T_s \sec\phi + L)}\,dx + s_+ \quad (13)$$

The groove surface temperature, T_s and the slope ϕ along the y direction are both functions of x and y. A general solution for groove shape requires that ϕ and T_s be determined. However, the centerline change in groove depth (where y=0 and ϕ=0) can be calculated. The incremental depth increase is:

$$\Delta D = \frac{a\pi^{1/2}P}{\rho v d\,(2c_p T_s + L)} = \frac{1.772\,aP}{\rho v d\,(2c_p T_s + L)} \quad (14)$$

With this analytical approach, a maximum groove depth can be found without resorting to iterative numerical methods.

EXPERIMENTAL PROCEDURE

In the single-beam experimentation, the cutting beam (TEM_{00} mode) was supplied by a 750W CO_2 laser and directed through an optical assembly to a focusing lens (0.1524m focal length). A focused spot with a 0.178mm diameter was generated. A cylindrical composite workpiece was held by a three-jaw chuck on a control table with automated x, y, and Θ stages. A 20psi N_2 coaxial jet was used in all experiments. Grooving experiments were conducted using beam power levels from 200W to 500W, radial scanning velocities from 2 to 10cm/s, and 1, 2, and 5 beam passes. Axial grooving tests were also conducted for glass/polyester samples at scanning velocities between 1 and 13cm/s for one pass.

Three composite materials were used in the grooving experiments. The carbon/teflon and glass/teflon composites consisted of 25% by volume short carbon and glass fibers in random orientation embedded in a teflon (polytetrafluoroethylene) matrix. The short fiber materials exhibited material properties largely independent of cutting direction due to random fiber orientation. This was consistent with the homogeneous properties assumption in the grooving model. The glass/polyester composite consisted of 50% by volume longitudinal glass fibers embedded in a polyester matrix. Glass/polyester was used to test the effects of cutting direction on depth and surface parameters. Thermal properties of the test materials are shown in Table 1.

An energy density parameter was used to incorporate all process conditions into one variable [2,3,4]. This parameter relates the total amount of energy received by a unit groove surface area to machining parameters. The energy density relationship is:

$$ED = \frac{P\lambda}{vd} \quad (15)$$

Measurements of groove depth, groove width and width of damage were taken for each cut. Groove depth was measured from the material surface to the innermost point of material damage (including both material ablation depth and inner heat affected zone). Groove width measurements were taken 0.152mm from the groove entrance and at the midpoint of groove depth. Damage width measurements, incorporating matrix charring and recession effects, were taken at 3 locations for each cut: 0.152mm from the groove entrance (outer), midpoint of groove depth (middle), and groove bottom (inner). Groove depth, width and damage width measurements were nondimensionalized with respect to spot diameter.

	Density (g/cm3)	Specific Heat (J/kg-K)	Thermal Conduct (W/m-K)	Thermal Diffusivity (m2/s)	Vapor Temp (deg C)	Heat of Vap (J/g)
Fiber Material:						
Carbon	1.85	710	50	3.8066E-05	3300	43000
Glass	2.55	850	1	4.6136E-07	2300	31000
Matrix Material:						
Teflon	2.32	929	0.35	1.6239E-07	312	1743
Polyester	1.25	1200	0.2	1.3333E-07	500	1000
Composite Material:						
Carbon/Teflon	2.2	874	12.7625	6.6375E-06	1059	12057
Glass/Teflon	2.37	909	0.5125	2.3789E-07	1082	9057
Glass/Polyester	1.9	1025	0.6	3.0809E-07	1400	16000

Table 1: Thermal Properties for Composite Materials

EXPERIMENTAL RESULTS

Carbon/Teflon

The plot of nondimensional depth versus energy density is shown in Figure 2. Groove depth showed a linear relationship (in log-log scale) with energy density. The larger variation of data in the low-end region of the plot is

attributed to the accuracy of the rotational axis motor operating at high speeds. A comparison with analytical model predictions showed less than one standard deviation difference between model prediction and experimental results for all test parameter values.

The groove widths increased almost linearly (in log-log scale) with energy density increase. Large data scatter was found wherever energy density was varied through changes in beam power. For a given ED/d value, minimum groove width at both groove entrance and midpoint regions was achieved through a combination of low power and high number of passes.

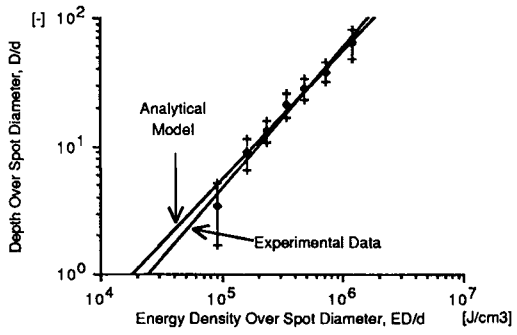

Figure 2: D/d vs ED/d for Carbon/Teflon

One useful result of the groove width data is a comparison with the criteria proposed in CIRP for surface quality classification [7], which specified 0.25mm and 0.5mm kerf widths for Class I and Class II surfaces, respectively. The only experimental condition that yielded a Class I cut was P=100W, v=10cm/s, and λ=1. Class II quality criterion was achieved for beam powers from 100W to 300W for all speeds and beam passes, as well as P=500W, λ=1, and all v. This implies that Class I criterion can be achieved with a combination of low power, high scanning velocity and high number of passes that yield ED/d values below $8x10^4J/cm^3$. Class II criterion can generally be achieved for ED/d values below $2x10^5J/cm^3$.

Glass/Teflon

A plot of nondimensional groove depth vs energy density for glass/teflon is shown in Figure 3. The groove width relationship with energy density followed similar trends as the results for carbon/teflon. Due to the short-fiber structure of the teflon composites, matrix recession was not detected. No evidence of surface charring was observed. This is attributed to the thermoplastic characteristic of teflon. Thus the only surface quality criterion for teflon composites is the kerf width. Groove width comparison with surface quality criteria yielded no data points satisfying Class I requirements. Class II criterion was satisfied using experimental conditions of P=200W with λ=1 and λ=2 and P=300W with λ=1 and λ=2. Generally, a Class II groove width can be produced with ED/d values below approximately $2x10^5J/cm^3$. Class I surfaces are expected to require ED/d values under $4x10^4J/cm^3$.

Glass/Polyester

A comparison of nondimensional groove depth and energy density for radial and longitudinal cuts, shown in Figure 4, showed that the analytical model overestimated D/d values for both cases. A model vs experimental difference within one standard deviation was reached only for ED/d values below $7x10^4J/cm^3$ for longitudinal cuts.

The relationship between groove width and energy density showed results similar to the teflon-matrix composites. A comparison of damage width criteria [7] (specifying damage widths of 0.2mm and 0.4mm for Class I and Class II

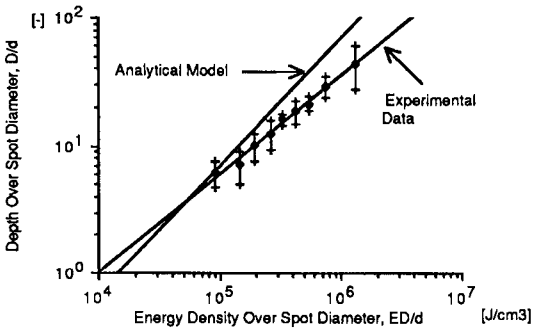

Figure 3: D/d vs ED/d for Glass/Teflon

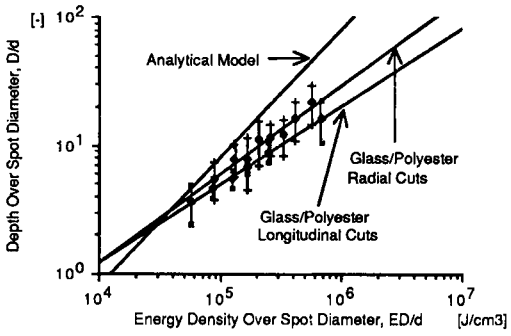

Figure 4:D/d vs ED/d for Glass/Polyester

surfaces, respectively) with glass/polyester results showed that Class I surface requirement was met in all cases except for high power, low speed cases. The groove entrance region showed the least material damage in most cases, while the groove bottom region showed the largest damage width values. Class II surface requirements were met by all experimental conditions. ED/d values under $2x10^5J/cm^3$ should produce a Class I surface. Comparison of damage width results with surface quality requirement for longitudinal cuts showed improvement over radial cuts.

DISCUSSION

Analysis of experimental data in Figures 2, 3, and 4 show variations in relationship slope that deviate from the analytical model. The model produces shifts in curve magnitudes for changes in material properties (such as ρ, c_p, or L) and predicts a set of three parallel lines with slope of 1 for the three materials. However, the analytical model does not account for the effects of heat losses to the environment. This heat loss effect is not significant in materials with a high thermal diffusivity (such as carbon/teflon) but becomes important for materials with low thermal diffusivities (such as glass/teflon and glass/polyester). The model prediction for groove depth (Eq. (14)) can be written in log-log form as:

$$\log(D/d) = \log(ED/d) + \log(a\pi^{1/2}d/(\rho(2c_pT_s + L))) \quad (16)$$

where the second right hand side term is constant for a given material.

Due to heat loss effects, glass/teflon and glass/polyester results show depth vs energy density relationships that are significantly lower in slope than model predictions. The experimental data can be described by an equation of the form:

$$\log(D/d) = n\log(ED/d) + \log(a\pi^{1/2}d/(\rho(2c_pT_s + L))) + C \quad (17)$$

where n is the slope of the linear log-log correlation (n=0.77 for glass/teflon and n=0.73 for glass/polyester) and C is a heat loss term. In modelling material depth response to energy density, values of n=1 and C=0 can be used for mate-

rials with thermal diffusivity values above approximately $10^6 m^2/s$, while $n<1$ and $C\neq 0$ for materials with thermal diffusivity values below $10^6 m^2/s$.

Figure 4 also shows the difference in slopes due to the effects of beam scanning direction for glass/polyester. This difference can also be related to the effects of heat losses to the environment. For longitudinal cuts, the matrix material at the surface is quickly vaporized by the beam, and a groove surface composed essentially of glass fibers is exposed. Due to the low thermal diffusivity of glass, the convective loss effect is significant. For radial cuts, the groove surface is composed of a heterogeneous mixture of glass fiber tips and matrix material. The volume-average thermal diffusivity of this mixture is higher than the value for glass, and heat loss effects are less pronounced than in the longitudinal cut cases. This phenomenon results in a steeper slope for the radial cuts in Eq. (17).

Benchmark ED/d values to achieve Class I and Class II surfaces can be determined from groove width comparisons. Due to large data scatter, these values give rough estimates of required operating conditions. For carbon/teflon, maximum ED/d values of $9x10^4 J/cm^3$ and $4x10^5 J/cm^3$ are required for Class I and Class II surfaces. These values are slightly lower for glass/teflon. Glass/polyester requires maximum ED/d values of $3x10^4 J/cm^3$ (Class I) and $1.3x10^5 J/cm^3$ (Class II) for longitudinal cuts. Radial cuts requires 50% smaller energy density values to meet surface quality criteria.

CONCLUSIONS

After examining the test data and the analytical model predictions, several conclusions can be drawn. First, although the energy density parameter is effective in characterizing groove depth, ED/d alone can only give rough estimates in specifying surface quality conditions. In order to improve the accuracy of surface quality predictions, specific operating parameters (scanning velocity, scanning direction, beam power and number of passes) must be noted. Generally, low power, high speed conditions minimize groove width and damage width. Second, all materials exhibited a linear (in log-log scale) relationship between groove depth and energy density for the range of process parameters tested. For carbon/teflon, the linear relation has a slope of 1. Due to the increased presence of convective loss effects, the slope for glass-fiber composites was significantly less. Heat losses also contributed to a difference in slope between radial and longitudinal cuts in glass/polyester. Third, the analytical model predicts groove depth for carbon/teflon to within one standard deviation for the entire test range of energy density. Since the analytical model did not account for heat loss effects, poor model/data agreement for glass-fiber composites was found for ED/d values above $2x10^5 J/cm^3$. Correction for convective losses resulted in an analytical solution in the form of Eq. (17).

These conclusions suggest several implications for the proposed three-dimensional laser machining process. The volume of material removed for each pass can be predicted from the energy density. The dimensional accuracy and finish of the resulting surface, however, cannot be accurately predicted by ED/d alone. By controlling specific parameters within ED/d (beam passes using high v and high λ values), surface quality can be controlled.

ACKNOWLEDGEMENTS

The work presented in this paper has been partially funded by the National Science Foundation (N.S.F. Grant DMC-8608273), Ford Motor Company, and Coherent General, Inc.

REFERENCES

1. Chryssolouris G., "Stock Removal by Laser Cutting", U.S. Patent No. 4,625,093., November 25, 1986.

2. Chryssolouris, G., Bredt, J., Kordas, S., and Wilson, E., "Theoretical Aspects of a Laser Machine Tool", ASME Winter Annual Meeting Proceedings, PED 20, Dec. 1986, pp. 177-190.

3. Chryssolouris, G. and Choi, W.C., "An Analysis of the Laser Grooving Process", to be published.

4. Chryssolouris, G. and Choi, W.C., "Theoretical Aspects of Laser Grooving", Proceedings, 14th Conference on Production Research and Technology, 1987, pp. 323-331.

5. Coherent, Inc., Engineering Staff, Lasers, Operation, Equipment, Application, and Design, 1980.

6. Clark, B. L., "A Parametric Study of the Transient Ablation of Teflon", ASME report no. 72-HT-32, Aug. 1972.

7. Konig, W. "Provisional List of Terms for Laser Beam Cutting", CIRP cooperative work, Jan. 1987.

8. Konig, W., Wulf, Ch., Grab, P. and Willerscheid, H., "Machining of Fiber Reinforced Plastics", Annals of the CIRP, Vol. 34/2, 1985, pp. 537-548.

9. Modest, M. F. and Abakians, H., "Evaporative Cutting of a Semi-Infinite Body With a Moving CW Laser", ASME Journal of Heat Transfer, Vol. 108, Aug. 1986, pp. 602-607.

10. Modest, M. F. and Abakians, H., "Heat Conduction in a Moving Semi-Infinite Solid Subjected to Pulsed Laser Irradiation", ASME Journal of Heat Transfer, Vol. 108, Aug. 1986, pp. 597-601.

11. Tagliaferri, V., Di Ilio, A. and Crivelli Visconti, I., "Laser Cutting of Fiber-Reinforced Polyesters", Composites, Vol. 16, No. 4, Oct. 1985, pp. 317-325.

12. Van Cleave, R., "Characteristics of Laser Cutting Kevlar Laminates", DOE Report No. BDX-613-2075, Jan. 1979.

13. Van Cleave, R., "Laser Cutting of Kevlar Laminates", DOE Report No. BDX-613-1877, Sept. 1977.